

Structural Characterization of Cu- 13.58%Al- 3.94%Ni (wt. %) shape memory alloy elaborated by fusion

S. Zeghdane, K. Necib, A. Britah

Laboratoire Génie des Matériaux, EMP, BP 17 Bordj El Bahri, Alger, Algerie

Abstract. This work concerns the structural characterization of Cu -13.58% Al- 3.94% Ni (wt. %) shape memory alloy elaborated by fusion using various techniques such as microscopy (OM and SEM), dilatometry and diffractometry (XRD). A particular attention is lent to the thermo elastic transformation may occur depending on the content of alloying and heat treatments' adopted. In this context, measurements of transformation temperatures were carried out. The microscopy is used for the characterization of alloy after different heat treatments adopted taking into account also the chemical composition. X-rays diffraction is used in order to access information on the different phases obtained and identify some types of martensite formed after quenching of alloy. The transformation temperatures are measured by the dilatometric analysis technique. This allows studying the structural evolution that occurs during heating and cooling of the alloy studied.

1. Introduction

Shape memory alloys, most often rated SMA, exhibit thermomechanical remarkable properties as the superelastic effect, the shape memory effect and two-way shape memory effect; these last two are probably the best known makes this class of materials very suitable for innovative applications in various fields. [1, 2]

These remarkable properties are controlled by a reversible displacive structural transformation, martensitic transformation, between solid phases: the highly symmetric austenite (A) and the less ordered martensite (M). The displacive character is dominated by shearing system of austenite and resulting transformation is controlled by the strain energy. Thus, for a given chemical composition of alloy, the characteristics of this transformation depend on the microstructure and consequently the conditions of elaboration and the thermomechanical history of material. [1, 2]

Our study focuses on the characterization of Cu-Al-Ni ternary SMA elaborated by fusion using various techniques such as microscopy, dilatometry and diffractometry.

2. Conduct of the study

The objective of this study is essentially, development and characterization of ternary Cu-Al-Ni shape memory alloy ternary Cu-Al-Ni. Figure 1 shows the conduct of this study:

e-mail: said_zeghdane@yahoo.fr

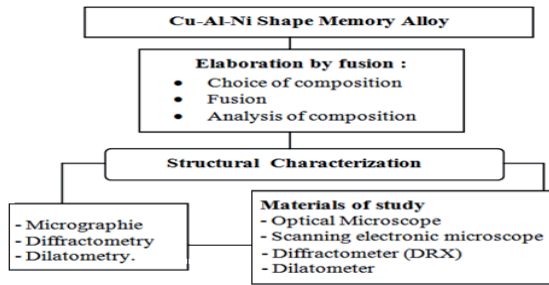


Fig. 1. Conduct of study

3. Elaboration of alloy

In preparing our alloy we must consult the equilibrium diagram of binary Cu-Al (Figure 2). The β phase stable at high temperatures transforms at $570\text{ }^{\circ}\text{C}$ to α ductile phase and γ_2 very fragile one. Rapid cooling from the stable zone of β phase can keep it in the metastable state, it is transformed into martensite at relatively high temperatures, the alloy having β phase the most stable (eutectoid composition of 24 atomic % or 11.8% by weight of aluminum) is transformed to martensite at $400\text{ }^{\circ}\text{C}$ after it is ordered DO3 to $550\text{ }^{\circ}\text{C}$ (Figure.2). For a temperature M_s near ambient temperature, requires a concentration about 14% by weight of aluminum for this value, it is virtually impossible to obtain β phase free of γ_2 phase (very fragile) and the alloy will be unusable. [1,3]

The addition of nickel moves the stability field of β to higher concentrations of aluminum and changes very little M_s Temperature curve. (Figure 3)

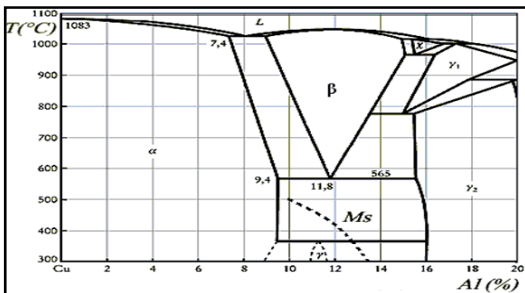


Fig. 2. Phase Diagram of Cu-Al with the evolution of M_s and DO3 order temperature. [3]

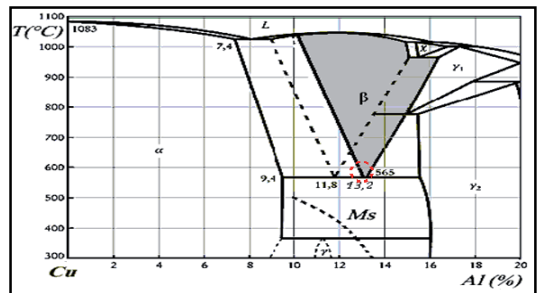


Fig. 3. Equilibrium diagram for Cu-Al showing the stability zone of β phase. The addition of Ni shifts the stability zone of β to high percentages in Al [3]

For example, the eutectoid composition goes to 13.2% by weight of aluminum to a concentration of 4% of nickel; the same M_s Temperature is about $150\text{ }^{\circ}\text{C}$. When the concentration exceeds 5% nickel, new precipitated Ni-Al appear: for common alloys are therefore limited to 3-4% nickel. The alloys used for applications are for 4% of nickel between 13 and 14% aluminum and correspond respectively to M_s Temperatures of $200\text{ }^{\circ}\text{C}$ and $50\text{ }^{\circ}\text{C}$ approx. [3]

3.1 Choice of composition

In theoretical approach we have seen that the martensitic transformation is generally characterized by a transformation temperature M_s , related to the composition of alloy. Experimentally, metallurgists have attempted to establish optical empirical relationships to predict the levels of the respective components of the alloy through the desired start point M_s and processing reports of levels of alloying elements to the content of basic element, in our case copper is the basic element. Our

choice was made to obtain a copper ternary shape memory alloy (Cu-Al-Ni) with a starting temperature of transformation M_s not to exceed 200 °C. For Cu-Al-Ni, as reported levels of alloying elements to the content of the base element (Cu) and the starting point of transformation M_s , the calculation gives the composition (in wt%) next: Cu - 14 Al - Ni 4 ($M_s \approx 190$ °C) [4, 5]

The metal used for making alloys are: The pure copper taken from plumbing pipe, pure aluminum cut from a sheet into small pieces and nickel powder very fine. The purity of these elements is acceptable to develop an alloy that can have a good memory effect.

3.2 Elaboration by fusion

The technique of preparation adopted is illustrated in Figure 4. The specimens were made following dimensions: length 130 mm, 14 mm in diameter. The samples studied are pellets (14 mm diameter, 3 mm thick).

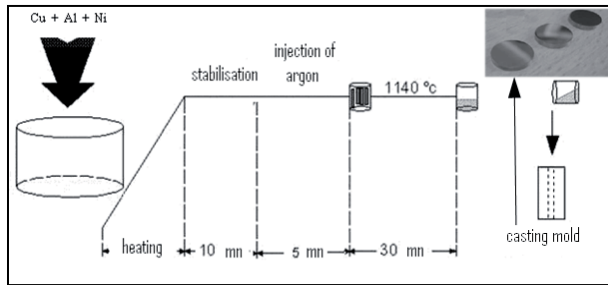


Fig. 4. Procedure for preparing the alloy [2, 3].

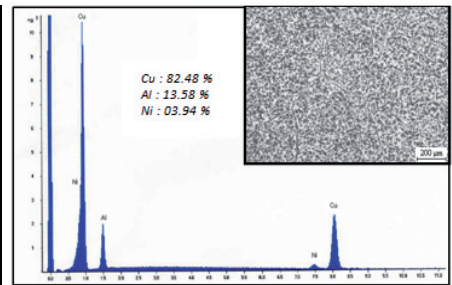


Fig. 5. Analysis of composition

3.3 Analysis of composition

The elaborated samples were subjected to an analysis of composition (Cu, Al, Ni) operated by a microanalyzer RONTEC mounted on the SEM. Example of analysis in Figure 5.

The analytical results seem different from one sample to another because the conditions of preparation (oxidation of Al and much more that of Cu). However we must also point out that these levels vary from one point to another, this always comes back to time keeping in the oven during the merger which determines the homogeneity of the diffusion phenomenon. For this, we have chosen samples which have compositions closer to those introduced: Al Cu -13.58% -3.94% Ni

4. Structural characterization

4.1 Optical microscope observations

4.1.1 Study of the initial-state

Before any observation, the samples were coated, polished mechanically and chemically attacked by a reagent composed of ferric chloride ($FeCl_3$), hydrochloric acid (HCl) and ethanol. The observations made in the raw state (as successor to the merger) for various magnifications are shown in Figure 6. The sample structure consists of γ_2 and α phases. γ_2 phase consists of irregular geometry and proportion increasingly important.

4.1.2 Study of the quenched-state

To detect the temperature of betatisation (having stabilizing the β phase at ambient temperature) and check the keeping time gives the largest amount of martensite, we realized the following treatments:

- We took five samples, numbered from 1 to 5, and then made a series of quenching in water at 25 °C of 850, 880, 910, 940, 970 °C with retention of 30 mn.
- For the five samples, we redid the hardening at 940 °C with maintain that vary from 10 mn to 50 mn with a step of 10 mn.

The test results give the temperature of 940 °C which gives the greatest amount of metastable β phase at ambient temperature and 30mn which gives the greatest amount of martensite. The structure of the quenched-state sample shows the existence of martensite in the needles form.

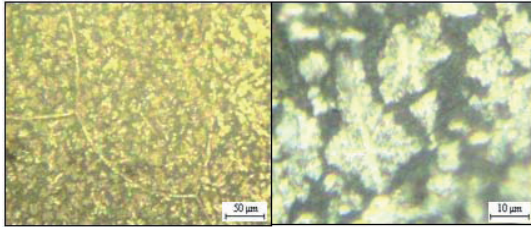


Fig. 6. Structure of sample. (Initial-state)

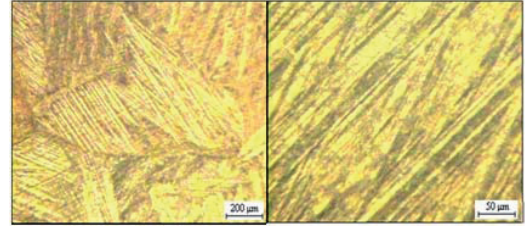


Fig. 7. Structure of sample. (Quenched-State)

4.5 Diffractometry (XRD)

All spectra were performed on a diffractometer XRD 3003 TT mount. The monochromatic X-radiation is produced by a copper anti-cathode rays which $K\alpha_1$ (1.5406 Å) and $K\alpha_2$ were isolated by discontinuous absorption through a nickel filter. ($V = 40\text{kV}$ and $I = 30\text{ mA}$). The XRD was conducted on pellets coated. The diagrams were recorded for 2θ values between $30^\circ - 60^\circ$ to observe the maximum of the main peaks. The scan speed used was set at $0.05^\circ / \text{s}$. [6]

- *Structure in initial state:* The diffraction analysis shows the existence of two phases (α and γ_2) and for our alloy, peaks related to the γ_2 phase are more intense than the peaks for α phase. [2]

- *Structure in quenching state:* The diffraction analysis shows that the martensite formed after quenching samples is β'_1 type. [2]

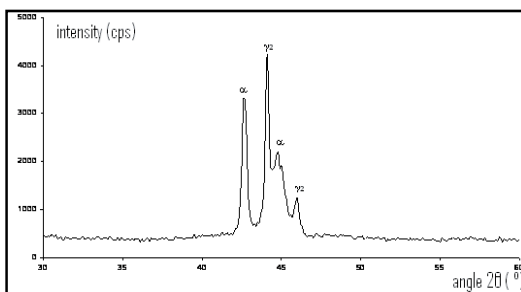


Fig. 8. XRD spectra. Initial-state

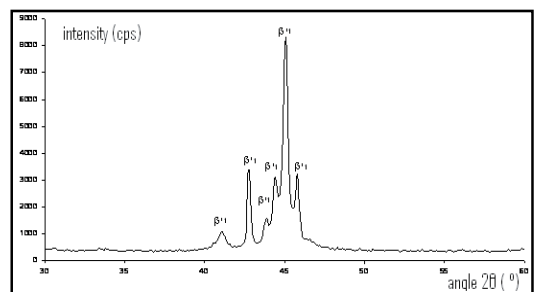


Fig. 9. XRD spectra. Quenched-state

4.6 Dilatometry

To study the structural evolution and determine the transformation points during heating and cooling of alloy, we used the dilatometric analysis technique. Indeed, a dilatometer Dil 801 which operates in a temperature range of 20 to 1500 °C and controlled speed between 1 and 30 °C/mn is used with cylindrical specimens (50mm long and 5mm in diameter). The linear deformation is detected by a sensor with a silica rod. The temperature is measured using a thermocouple placed near the sample. The measurements are recorded by computer.

It was established variation curves of elongation versus temperature T. This quantity is very important to follow because any change of phase so of structure results in a change of length δL . A change of structure is associated with a change in the apparent coefficient of linear dilatation is reflected on the dilatometric curves by a change of slope. Thus the transformation points are determined on the locations or the curve changes slope and hence the interest to have the curve derived in order to clarify these points. [2, 7]

4.6.1 Evolution of quenched structure

The sample was treated for 30 mn at 940 °C and then quenched in water at 25 °C.

To study the structural evolution that occurs during heating and cooling of our sample, we used a heating speed $V_c = 5 \text{ }^\circ\text{C}/\text{mn}$ until a temperature of β phase field (800 °C) monitoring of cooling at the same speed $V_r = 5 \text{ }^\circ\text{C}/\text{mn}$ until the ambient temperature t. The dilatometric curves obtained are given by figures.10;

To determine the transformation points, we used the tangent method to determine these points by intersection of tangents at inflection points of the peak with the baseline extension. (Figure 13)

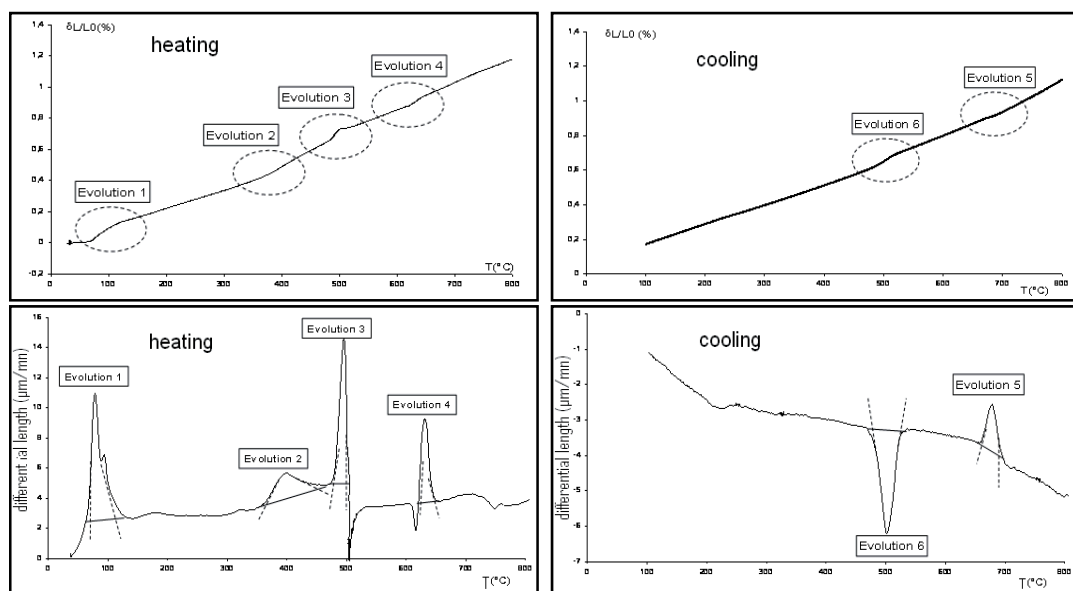


Fig. 10. Presentation of different transformations

- **Evolution 1:** in [25-250] °C, show the transformation of t martensitic phase to prémartensitique phase R. (As: 70 °C, Af: 106 °C)

Evolution 2: in [350-450] °C, leads to the formation of coherent precipitates in the matrix alloy and rich in nickel and aluminum. (Start: 363 °C, end: 434 °C)

Evolution 3: in [450-550] °C, corresponds to the stripping of previously formed and precipitated the breakdown of the R phase in equilibrium constituents (α and γ_2). (Start: 470 °C, end: 492 °C)

Evolution 4: in [550-700] °C, corresponds to the recombination of constituents to form the equilibrium β phase stable. (Start: 610 °C, end: 635 °C)

Evolution 5: in [750-600] °C, corresponds to the transformation of β phase to β phase + forming an equilibrium (α or γ_2). (Start: 679 °C, end: 647 °C)

Evolution 6: in [600-450] °C corresponds to the transformation of β phase to ($\alpha + \gamma_2$) phase. (Start: 540 °C, end: 437 °C)

4.6.2 Influence of heat treatments

To study the effect of heat treatments on these evolutions, we conducted the following treatments:

Table. 1. Heat treatments adopted

State	Heating T.(°C)	Time Keeping. (mn)	Cooling medium
1, 2	940	30	Water at. 25 °C, water at. 00°C
3	940	30	Oil at. 25°C
4	940	15	Water at. 25 °C
5	900	30	Water at. 25 °C
6	900	15	Water at. 25 °C

The dilatometric curves (with a speed $V_c = V_r = 5 \text{ } ^\circ\text{C} / \text{min}$) have the same manners in all cases described in the table (Table.1) with the presence of the same changes described in the preceding paragraph. The only difference observed concerns the differential length of the inverse transformation represented by variations in peaks height. (Figure 11)

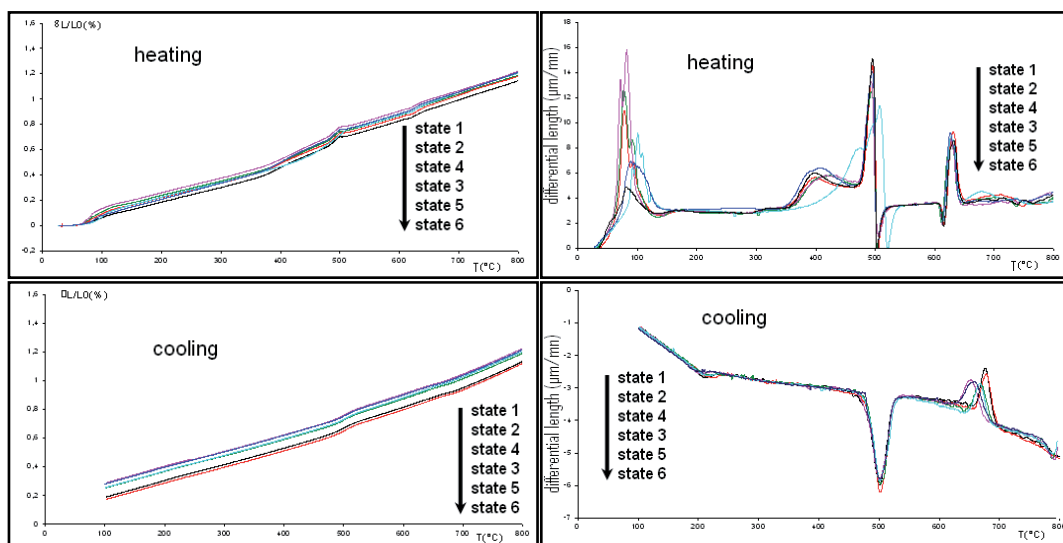


Fig. 11. Dilatometric curves during heating and cooling.

4.6.2 Influence of heating temperature and time keeping

The transformation points of each evolution are determined by the tangents method and the results obtained are given in the following table:

Table. 2. Transformation points. State 1, 4, 5 et 6

	Evolution 1		Evolution 2		Evolution 3		Evolution 4		Evolution 5		Evolution 6	
	A_s	A_f	Start	end	Start	end	Start	end	Start	end	Start	end
state 1	65	102	366	448	175	503	613	645	672	624	538	472
state 4	66	106	365	443	478	505	616	646	692	656	538	472
state 5	72	121	363	445	474	505	615	644	680	628	538	472
state 6	67	112	366	444	473	505	614	644	690	654	538	472
	Evolution 1		T° summit of peak (°C)		$\delta L/L0$ (%)		Dilatation speed ($\mu\text{m}/\text{min}$)		Dilatation coef. ($10^{-6}/^\circ\text{C}$)			
state 1	65	102	80		0.073		14.75		13.24			
state 4	66	106	79		0.041		10.8		7.88			
state 5	72	121	95		0.075		7		10.60			
state 6	67	112	80		0.031		4.9		5.63			

- **State 1 and 5:** Note that the transformation points, the speed of dilatation and coefficient alpha are different. The dilatation in state 1 is 0.0007 obtained with a speed 14.75 $\mu\text{m}/\text{mn}$, by cons in state 5, the dilatation is the same but it is obtained with a speed of 7 $\mu\text{m}/\text{mn}$. Therefore, the transformation of austenite to martensite is also quick in state 1 than state 5

- **State 4 and 6:** The dilatation in state 4 is 0.0004 obtained with a speed of 10.80 $\mu\text{m} / \text{mn}$, by cons in the state 6, it is 0.0003 obtained with a speed of 4.9 $\mu\text{m} / \text{mn}$. Therefore, the transformation of austenite to martensite is also quick in state 4 than state 6.

The same remarks in state 1, 4 and state 5, 6, Show that it is an influence of heating temperature and keeping time on this transformation.

4.6.3 Influence of cooling medium

The transformation points of each evolution are determined by tangents method and the results obtained are given in the following table 3:

Table. 3. Transformation points (state 1.2 and 3)

	Evolution 1		Evolution 2		Evolution 3		Evolution 4		Evolution 5		Evolution 6	
	A _s	A _f	Start	end								
state 1	65	102	366	448	175	503	613	645	672	624	538	472
state 2	66	104	368	449	476	504	612	646	682	646	538	472
state 3	87	121	468	481	487	522	616	145	683	645	538	472

	Evolution 1		T° summit of peak (°C)	$\delta L/L_0$ (%)	Dilatation speed ($\mu\text{m}/\text{min}$)	Dilatation coef. ($10^{-6}/^\circ\text{C}$)
	A _s	A _f				
state 1	65	102	80	0.073	14.75	13.24
state 2	66	104	78	0.048	12.65	10.06
state 3	87	121	100	0.074	9	9.73

From these results, we note that the transformation points in state 3 are moving to higher values compared to state 1 and 2. The dilatation obtained with different speeds varies from one state to another. So, the cooling medium influences the formation of martensite, which transforms to austenite with different transformation points.

4.6.4 Determination of transformation points (A_s, A_f, M_s and M_f)

To determine the points of beginning and end of the martensitic transformation, we performed thermal cycles by dilatometry at a speed of 5 °C / min to highlight the different transitions expressed between ambient and 700 °C. This sample was treated to the threshold of each evolution 1, 2, 3 and 4; either, 200, 450, 550 and 700 °C, then cooled at the same speed. (Figure 12, Table 4).

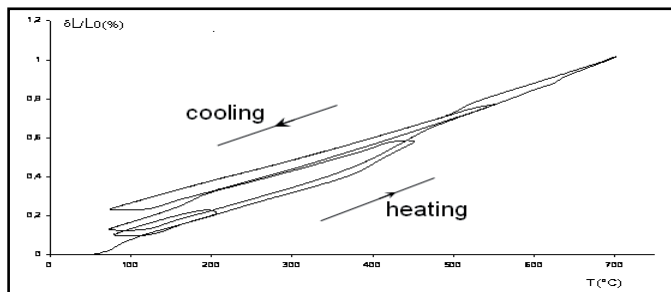


Fig. 12. Thermal cycles performed.

According to this curve, we note that there are several changes and to better explain them; using the differential length curves shown in Figure 16.

Table. 4. Transformation points measured during thermal cycling

	Transformation points	Heating at 200°C	Cooling from 200°C heating at 450°C	Cooling from 450°C heating at 550°C
Transformation M → A	A _s (°C)	80	134	152
	A _f (°C)	110	164	198
Transformation A → M	M _s (°C)	/	140	156
	M _f (°C)	/	123	128

- *Heating at 200 ° C after quenching*: curve (a) of Figure 13; the transformation at heating is $\beta_1 \rightarrow \beta_1$ and manifested by a peak which shows a maximum dilatation speed.

- *Cooling from 200 ° C and heating to 450 ° C*: cooling the sample from 200 ° C shows the existence of a direct transformation $\beta_1 \rightarrow \beta_1$ and manifested by a peak when the dilatation speed decreases. In this case we can determine the points Ms and Mf.

When applying heating to 450 ° C, we observe that the points As and Af of the inverse transformation $\beta_1 \rightarrow \beta_1$ rise, and the presence of another transformation that begins at 370 ° C and finishes around 436 ° C. This evolution is the formation of coherent precipitates in the matrix alloy and rich in nickel and aluminum.

Measuring of M_s, M_f, A_s and A_f shows a behavior of type II.

- *Cooling from 450 ° C and heating to 550 ° C*: cooling the sample from 450 ° C shows the existence of a transformation of austenite to martensite with superior Ms and Mf points.

When applying heating to 550 ° C, we observe that As and Af of the inverse transformation rise, and the presence of another evolution that begins at 470 ° C and finishes around 500 ° C . This transformation led to the stripping of precipitates formed previously and decomposition of the β_1 phase in equilibrium constituents (α , γ_2).

- *Cooling from 550 ° C and heating to 700 ° C*: One comment on the curve (c') of Figure 13 may that any transformation during cooling from 550 ° C, those leading to the disappearance of the β_1 phase.

When applying heating to 700 ° C, we observe that there is an evolution starts at 612 ° C and finishes around 640 ° C. This transformation corresponds to the recombination of equilibrium constituents α and γ_2 to form the β phase stable.

- *Cooling from 700 ° C*: we observe a transformation that begins at 565 ° C and finishes around 482 ° C, corresponding to the eutectoid transformation of β phase to α and γ_2 phases.

5. Conclusion

For elaboration and characterization of alloy, it was based on two axes:

An axis for the elaboration of our alloy by melting, overseeing everything that can hinder this elaboration (heating conditions, cooling conditions and risk watching this elaboration as oxidation). In addition, there was broad interest in heat treatments to highlight the main characteristic of these alloys (martensitic transformation). However, this mode of elaboration was not without consequences on the morphology of grains. Indeed, their growing uncontrolled led us to consider some form of refining by heat treatment method (annealing regeneration).

A second axis for the structural characterization of alloy using several techniques, Microscopy allowed to observe the structure of this alloy and to access information on the different phases observed (α and γ_2) we used the X-ray diffraction and based on work in references [2, 6]. This technique can also determine a variant of martensite (β_1) formed after quenching. Finally, the dilatometric analysis technique permitted to determine the points of martensitic transformation and to study the various phase transformations that occur during heating and cooling of this alloy under conditions chosen.

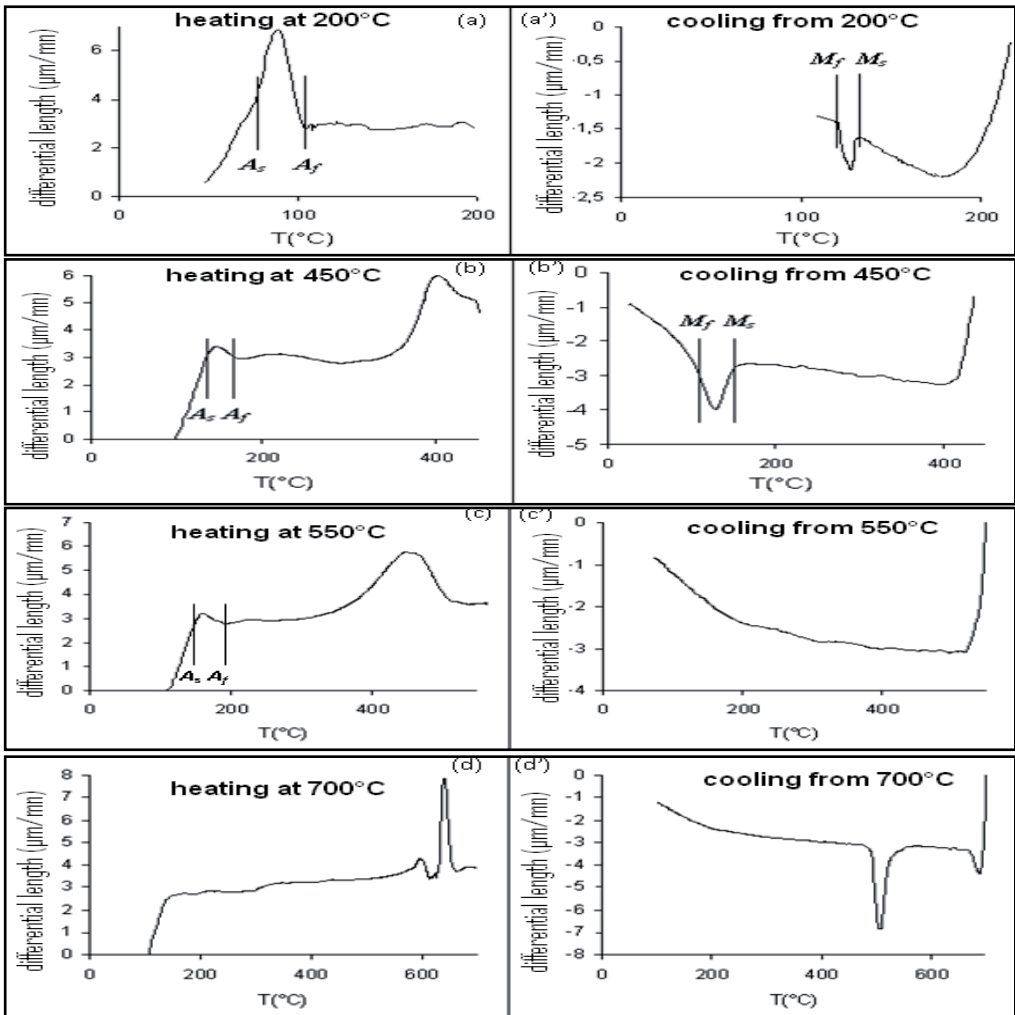


Fig. 13. Determination of transformation points.

References

1. E. PATOOR, *Technologie des Alliages à Mémoire de Forme*, Hermès, Paris, (1994)
2. M. BOUABDALLAH, *Elaboration et caractérisation des AMFs à base de cuivre de Cu-Al-Ni eutectoïdes*, Doctorate thesis, ENP, Alger, (1999)
3. C. SAIB, *Caractérisations Structurale et Mécanique des Alliages à Mémoire de Forme ternaires de types Cu-Al-Ni ; Cu-Zn-Al élaborés par Fusion*, 4th JM, EMP, Algérie, (2003)
4. G. CLEMENT, M. MUTUEL, J.M. WELTER, *Industrial processing of CuAlNi and its recent developments*, International Conference on Industrial Applications of SMA, Canada, (1994)
5. G. LOJEN, I. ANZEL, A. KNEISSL, A. KRIZMAN, *Microstructure of rapidly solidified Cu-Al-Ni SMA ribbons*, Journal of Materials Processing Technology, Slovenia, 220-229, (2005)
6. R. ZENGIN, M. CEYLAN, *Influence of neutron irradiation on the characteristics of Cu-13%wt.Al-4%wt.Ni shape memory alloy*, Materials Letters 58, 55- 59, (2003)
7. M. BOUABDALLAH, G. CIZERON, *Comportement des transformations thermoélastiques au cyclage en dilatométrie*, 1^{er} Congrès Interdisciplinaire sur les Matériaux, Tours, France, (2002).